Self-organized criticality induced by quenched disorder: experiments on flux avalanches in NbH$_x$ films.

M. S. Welling, C. M. Aegerter*, and R. J. Wijngaarden

Division of Physics and Astronomy, Faculty of Sciences, Vrije Universiteit, De Boelelaan 1081, 1081HV Amsterdam, The Netherlands

(February 2, 2008)

We present an experimental study of the influence of quenched disorder on the distribution of flux avalanches in type-II superconductors. In the presence of much quenched disorder, the avalanche sizes are power-law distributed and show finite size scaling, as expected from self-organized criticality (SOC). Furthermore, the shape of the avalanches is observed to be fractal. In the absence of quenched disorder, a preferred size of avalanches is observed and avalanches are smooth. These observations indicate that a certain minimum amount of disorder is necessary for SOC behavior. We relate these findings to the appearance or non-appearance of SOC in other experimental systems, particularly piles of sand.

PACS numbers: 05.65.+b, 74.70.Ad, 64.60.Ht, 74.25.Qt

Self-organized criticality (SOC) [1] has generated great interest over the last 15 years mainly due to its wide range of possible applications in many non-equilibrium systems [2,3]. However, progress has been hampered by the fact that clear, tell-tale signs of criticality, such as finite-size scaling in the distribution of avalanches, have only been observed in very few controlled *experiments* [4]. Recently however, there have been a number of experimental observations of criticality in both two- [5,6] and three dimensional systems [7–9]. However, the critical ingredients to obtain SOC in an experimental system still remain obscure.

Recent theoretical advancements have studied the nature of the criticality in SOC and made a link with phase transitions describing how a moving object comes to rest [10,11]. Such absorbing state phase transitions are closely related to the roughening of an elastic membrane in a random medium [12]. In these theoretical models, there needs to be an absorbing state phase transition underlying the process at hand in order to observe SOC. This critical state is reached by a self-organization process [13], which depends on slowly driving the system away from its state where everything is at rest. If the driving is not slow enough, the relaxations to the critical point may be disturbed by the driving, such that no critical state is reached [14]. Too strong driving may have occurred in some of the early experiments, particularly those performed in rotating drums and where the grains were dropped from a considerable height. The absence of an underlying phase transition, however, would be more fundamental and detrimental to SOC. In the case of absorbing state phase transitions, it is known that the presence of quenched disorder plays an important role in the nature of the critical point, such that this may also be an important ingredient in obtaining SOC behavior.

Here we present an *experimental* investigation of the influence of disorder on the appearance or non-appearance of SOC. Therefore it is necessary to have a system, where the quenched disorder can be experimentally changed while leaving all other aspects the same, as well as having a system which has been shown to show SOC at least in some circumstances. We study the avalanche dynamics of magnetic vortices in the type-II superconductor Niobium in the presence of Hydrogen impurities using magneto-optics. As first noted by de Gennes [15], the penetration of a slowly ramped magnetic field into a type-II superconductor has a strong analogy to the growing of a sand pile, the archetypal example of SOC. It has been shown in the past, that these vortex avalanches are distributed according to a power-law [16] and more recently that they obey finite-size scaling [9]. However, due to the presence of pinning in the system, studying magnetic vortices allows a detailed investigation of the influence of quenched disorder on their avalanche distribution and structure. Nb is particularly suited for this purpose, as it easily takes up H impurities (which locally destroy superconductivity, see below) [17], which can be added to the sample via a contact gas, thus allowing an experimental control of the amount of quenched disorder in the system. Furthermore, studying magnetic vortices has the advantage that kinetic effects in their dynamics, which are thought to have hampered some sand-pile experiments [5], are naturally absent due to the over-damped dynamics of the vortices [18].

The experiments described here were carried out on a Nb film of a thickness of 500 nm, evaporated under ultra high vacuum conditions on an 'R-plane' sapphire substrate. The films were then covered with a 10 nm Pd caplayer in order to facilitate the catalytic uptake of H into the film [19].

The local magnetic flux density, B_z, just above the sample is measured using an advanced magneto-optical (MO) setup, directly yielding the local Faraday-angle in an Yttrium-Iron Garnet indicator, using a lock-in technique [20]. Images are taken with a charge-coupled device camera (782×582 pixels) with a resolution of 3.4 μm per pixel. The sample is placed in a cryo-magnet and cooled to 4.2 K in zero applied field. The external field is then ramped from 0 to 20 mT in steps of 50 μT, where the flux in the sample is relaxed for 3 seconds before an MO

picture is acquired. This sequence is repeated twice for each H concentration to check for reproducibility.

The quenched disorder in the sample is increased after such a sequence of two field sweeps by equilibrating the sample with a certain higher partial pressure of H at room temperature for one hour. The partial loading pressures used in the experiments discussed here were 80, 260, 1130, and 1810 Pa. We estimate that the H impurities present in the as grown sample correspond to a partial loading pressure lower than roughly 10 Pa. After equilibration, ensuring a uniform distribution of H in the Nb film, the sample is cooled down again. In this cooling procedure, phase separation occurs in H-rich and H-poor regions [21], where superconductivity is suppressed in the H-rich phase [22]. Thus the clusters of H-rich phase, which are in the order of 0.1 to 1 μm in diameter [21], act as effective pinning sites for the vortices and thereby introduce quenched disorder.
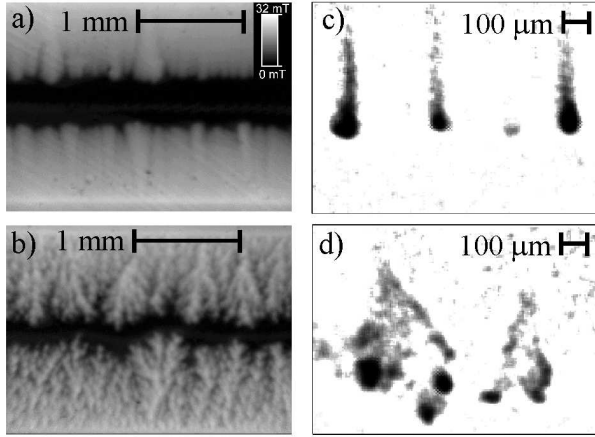

FIG. 1. a) The magnetic flux landscape in the center of the Nb film without added Hydrogen impurities. The magnetic flux density in the sample is indicated by the brightness, where white corresponds to 32 mT and black corresponds to 0 mT (see inset). b) The flux landscape in the same sample after the application of a H pressure of 1810 Pa at room temperature. As can be seen, the flux structures are much more disordered and branched. c) Magnetic flux avalanches in the absence of H treatment, as given by the subtraction of two consecutive MO images. Note that the magnification and the grey-scale is different from a), white corresponds to 0 mT and black corresponds to 3 mT. The avalanches have a predominant size and are rather smooth and plume-shaped. d) Flux avalanches after H treatment with 1810 Pa gas pressure at room temperature, again obtained from a subtraction of consecutive MO images (grey scale and magnification are as in c). The avalanches are more fractal and branched than in c) and do no longer have a preferred size (see text).

In this manner, we obtain a collection of magnetic flux landscapes as shown in Fig. 1a), which are then analyzed in terms of the avalanches that have occurred between time steps. In order to obtain the amount of magnetic flux that has been transported in one avalanche, we first average each image over a set of 4 × 4 pixels to reduce noise. Then two consecutive images are subtracted lead-

ing to an image like that shown in Fig. 1c). As can be seen in the figure, in each image we observe a number of avalanches. These are identified individually, using a threshold of 0.3 mT in ΔB_z. The amount of flux in each of these avalanches is subsequently determined from integrating the difference in flux density over the area of the avalanche:

$$s = \Delta\Phi = \int \Delta B_z dx dy. \qquad (1)$$

From the spatial resolution of the setup and the threshold level of the avalanche identification, we can determine the smallest avalanches that are still resolved to contain about 20 Φ_0, where $\Phi_0 = h/2e$ is the magnetic flux carried by each vortex. In order to check for finite size scaling, we discard avalanches exceeding a linear extent of 200, 100, and 50 μm from the analysis. This corresponds to decreasing the system size accordingly, as the linear extent of an avalanche cannot exceed the system size.

As can be seen in Fig. 1c), when the sample has not been treated with H, the avalanches have a characteristic structure and area. This leads to a peak in the size distribution, which disappears as avalanches exceeding the preferred linear extent are discarded. Thus in the absence of H-induced quenched disorder, no SOC behavior is observed, as there is no finite-size scaling of the avalanche distribution. This is shown in Fig. 2a), where we show the scaled avalanche size distribution for the sample without H treatment. Here, the size distribution has been logarithmically binned, such that avalanche size steps in the histogram are separated by a constant factor rather than a constant step width. Moreover, the histograms are scaled with s^τ, which leads to horizontal lines in case the avalanches are power-law distributed. The displaced flux per avalanche is scaled by L^{-D}, where L is the scale above which avalanches are discarded and D is the fractal dimension of the avalanches. In order to obtain the 'collapse' in Fig. 2a), we have used $\tau = 1.35$ and $D = 2.75$. The value of τ is determined from a best collapse of the data onto a horizontal line for small s. The value of D is found from the best collapse of the cut-off values. The nice collapse of cut-off values indicates that the avalanches in this case do have a definite fractal dimension, which is close to 3, as one would expect given their smooth appearance in Fig. 1c). The peak that can be observed in the distribution is due to the predominance of avalanches containing about $\sim 2500 \Phi_0$, which can also be inferred from Fig. 1c).

Turning to the data in Fig. 1d), it can be seen that in the presence of strong quenched disorder (i.e. after treating the sample with 1810 Pa of H gas), the avalanche structure is markedly different from that in the pristine case. Now, the flux moves in a much more branched way and furthermore a preferred size of avalanches is absent. Again, we have checked this with a finite-size scaling analysis of the avalanche size distributions, see Fig. 2b). The size distribution is again logarithmically

binned and scaled in order to obtain a curve collapse. Here, in contrast to Fig. 2a), there is good curve collapse and thus we can determine the size distribution exponent and avalanche dimension to be $\tau = 1.07(2)$ and $D = 2.25(5)$, where we observe a power-law distribution over more than two orders of magnitude.
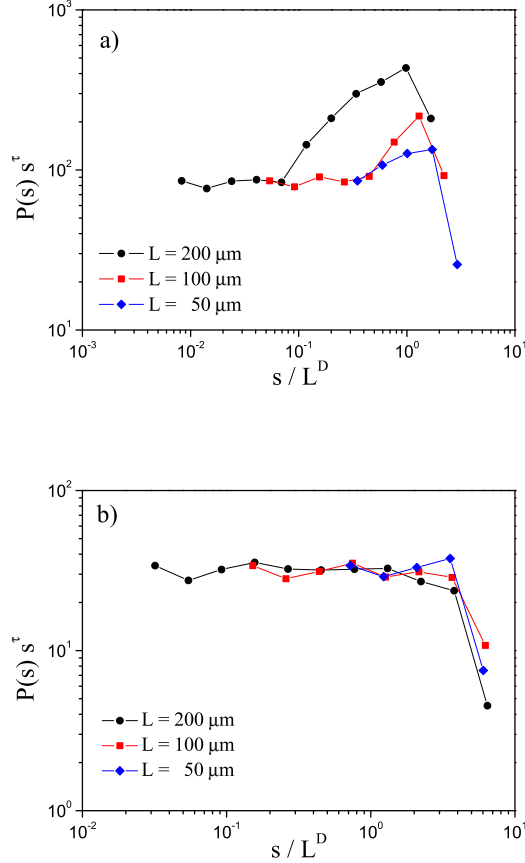

FIG. 2. a) The flux avalanche size distributions in the absence of Hydrogen treatment. Data are shown for sets of avalanches not exceeding different linear sizes of $L = 200$, 100, and 50 μm. The different distributions are vertically scaled with s^τ and the sizes are horizontally scaled with L^{-D}, in order to obtain the usual curve collapse for finite size scaling. However, as avalanches of $\sim$2500 Φ_0 are preferred, no good curve collapse is obtained in this region. For small avalanches and avalanches of the cut-off size, the curves do collapse, such that the fractal dimension of the avalanches can be determined. b) The avalanche size distributions scaled in the same way, for experiments after H treatment at 1810 Pa of the sample. Here a good curve collapse is observed, with power-law scaling over more than two decades. This is clear evidence that in the presence of quenched disorder, SOC is present in the vortex avalanches.

This overall behavior of flux avalanches in the presence of changeable quenched disorder has also been studied in molecular dynamics simulations of a collection of vortices [23]. This is a great advantage of the vortex system over the study of sand piles, as the interactions between vortices are well known [18] and can thus be simulated in order to separate collective effects from microscopic dynamics. In their study, Olson *et al.* [23] have found that on increasing the pinning density, the avalanche distributions change from showing a preferred size (with a power-law distribution at small sizes) to a power-law distribution. Furthermore, in the case of strong pinning, the exponent τ obtained in these power-law distributions is between 1 and 1.4 in very good agreement with our experimental values. Moreover, in molecular dynamics simulations, the movements of all vortices can be followed and it turns out that in the case of low pinning density, the avalanches form channels [23], which is highly reminiscent of the structures seen in Fig. 1c).

Let us now turn to the general implications on the appearance of SOC that can be drawn from the above observations. As we have shown, in the absence of quenched disorder, even the non-kinetic vortices [18] do not show finite-size scaling in their avalanche distribution. Furthermore, it has been shown previously that steel balls in a two dimensional pile can show SOC [6] when quenched noise is introduced via a fixed random arrangement of balls at the base. These two observations together seem to indicate that kinetic effects may be less important than previously thought [5], while it is the presence of quenched noise that leads to the appearance of SOC. This is also corroborated by molecular dynamics simulations on vortices, using over-damped dynamics finding the same result [23].

The importance of quenched disorder can be best seen in the structure of the avalanches, which is intimately connected to the surface of a pile or flux landscape [7,24]. As the number of pins is increased, the vortex avalanches have to accommodate to their presence. This frustration leads to a much more branched and open avalanche structure. This is shown in Fig. 3, where the circles show the values of D for different H loading pressures. As can be seen, at low pinning density, the avalanches have a dimension close to 3, indicating a smooth structure, whereas with increasing H content, the avalanche dimension decreases. Due to the more complex structure of an avalanche, a bigger range of possible avalanche sizes can be explored over the area of the sample. Thus there is no longer a preferred size of avalanches and hence SOC behavior occurs. Again, we can compare our results to those of Altshuler *et al.* [6], where in the absence of SOC, only a small part of the pile took part in avalanches and the pile surface overall was much smoother than in the case where SOC was observed.

In order to quantify the roughness [25] of the flux landscape, we determine the width, $\langle (B_z(x,y) - \langle B_z(x,y)\rangle_y)^2\rangle^{1/2}$, of the flux landscape after subtraction of the average profile, $\langle B_z(x,y)\rangle_y$. As can be seen in Fig. 3, with increasing H content, the flux landscape becomes more rough as given by a fourfold increase in surface width. Thus as has been observed in experiments using steel balls [6] as well as in rice piles [7,26], SOC be-

3

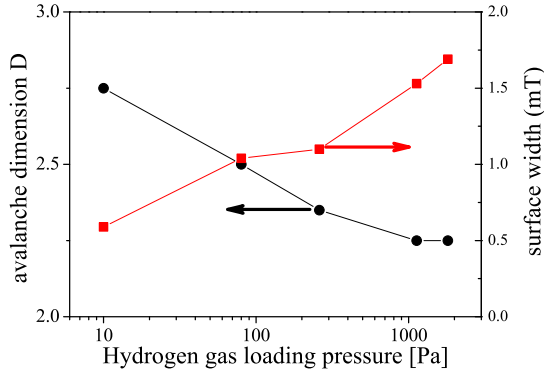havior in the flux landscape is coupled to the observation of a rough pile surface.

FIG. 3. The fractal dimension of the avalanches (circles) and the surface width (see text) of the flux landscape (squares) as a function of Hydrogen partial pressure. Data for the pristine films are shown at 10 Pa, the estimated maximum contamination H pressure. The fractal dimension decreases with increasing quenched disorder, corresponding to a more branched and rough structure, as seen in Fig. 1d). The surface width increases with quenched disorder, which indicates that the flux landscape becomes increasingly rough as H is introduced into the sample, as can be seen in Fig. 1b).

In conclusion, we have shown in the case of high pinning density that the magnetic flux avalanches observed in a Nb film show finite-size scaling, which implies the presence of SOC in the system. However, in the presence of a low pinning density, a preferred size of avalanches is found and no finite-size scaling is observed. This demonstrates the importance of quenched disorder in the system in order to obtain SOC behavior. The exact position of the transition from non-SOC to SOC behavior cannot be determined very accurately due to experimental limitations (e.g. 'noise' in Fig. 2 and limited accessible range of L), but might also be intrinsically smooth if one considers the gradual changes observed in Fig. 3 for the avalanche dimension D and surface width. Our *experimental* observation of this transition as a function of disorder is in agreement with previous numerical work on cellular automata [27] and with molecular dynamics simulations of magnetic vortices [23]. In addition, our findings are consistent with the point of view of SOC as an absorbing state phase transition [10,13]. In absorbing state phase transitions, such as directed percolation [25], the density of quenched disorder is a critical parameter, whereby a phase transition can be induced. The presence of such an underlying phase transition is a necessary condition in order to obtain SOC in the model of Vespigniani *et al.* [13]. Thus again, this view advocates that the increase of quenched noise can lead to the appearance of SOC, as indeed we have found experimentally.

* Present address: Fachbereich Physik, Universität Konstanz, P.O. Box 5560, 78457 Konstanz, Germany.
[1] P. Bak, C. Tang, and K. Wiesenfeld, Phys. Rev. Lett. **59**, 381 (1987) and Phys. Rev. A **38**, 364 (1988).
[2] P. Bak, *How nature works* (Oxford Univ. Press, 1995).
[3] H.-J. Jensen, *Self-Organized Criticality* (Cambridge University Press, 2000).
[4] see e.g. H. M. Jaeger, R. P. Behringer, and S. R. Nagel, Rev. Mod. Phys. **68**, 1259 (1996); S. R. Nagel, *ibid.* **64**, 321 (1992) and references therein.
[5] V. Frette *et al.*, Nature (London) **379**, 49 (1996).
[6] E. Altshuler *et al.*, Phys. Rev. Lett. **86**, 5490 (2001).
[7] C. M. Aegerter, R. Günther, and R. J. Wijngaarden, Phys. Rev. E **67**, 051306 (2003).
[8] R. M. Costello *et al.*, Phys. Rev. E **67**, 041304 (2003).
[9] C. M. Aegerter, M. S. Welling, and R. J. Wijngaarden, Europhys. Lett. **65**, 573 (2004).
[10] R. Dickman, *et al.*, Braz. J. Phys. **30**, 27 (2000); cond-mat 9910454.
[11] M. Paczuski, S. Maslov, and P. Bak, Europhys. Lett. **27**, 97 (1994).
[12] M. J. Alava and K. B. Lauritsen, Europhys. Lett. **53**, 563 (2001); G. Pruessner, Phys. Rev. E **67**, 030301 (2003).
[13] A. Vespignani and S. Zapperi, Phys. Rev. Lett. **78**, 4793 (1997); Phys. Rev. E **57** 6345 (1998); R. Dickman *et al.*, Phys. Rev. E **57**, 5095 (1998).
[14] G. Grinstein, J. Appl. Phys. **69**, 5441 (1991).
[15] P. G. de Gennes, *Superconductivity of metals and alloys* (Addison-Wesley, New York, 1966).
[16] S. Field, J. Witt, and F. Nori, Phys. Rev. Lett. **74**, 1206 (1995); C. M. Aegerter, Phys. Rev. E **58**, 1438 (1998); K. Behnia *et al.*, Phys. Rev. B **61**, R3815 (2000); E. Altshuler *et al.*, cond-mat/0208266.
[17] G. Alefeld and J. Völkl, *Hydrogen in Metals II, Topics in applied Physics vol. 29* (Springer, Heidelberg, 1978).
[18] G. Blatter *et al.*, Rev. Mod. Phys. **66**, 1125 (1995).
[19] M. S. Welling *et al.*, Physica C **406**, 100 (2004).
[20] R. J. Wijngaarden *et al.* Rev. Sci. Instrum. **72**, 2661 (2001).
[21] T. Schober, Phys. Stat. Solidi **30**, 107 (1975); K. Nörthemann *et al.*, J. Alloys Comp. **356-357**, 541 (2003).
[22] E. G. Maksimov and O. A. Pankratov, Usp. Fiz. Nauk **116**, 403 (1975); L. Ya. Vinnikov *et al.*, Sov. J. Low Temp. Phys. **3**, 4 (1977).
[23] C. J. Olson, C. Reichhardt, and F. Nori, Phys. Rev. B **56**, 6175 (1997).
[24] M. Paczuski, S. Maslov, and P. Bak, Phys. Rev. E **53**, 414 (1996).
[25] A. L. Barabasi and H. E. Stanley *Fractal Concepts in Surface Growth* (Cambridge University Press, 1995).
[26] A. Malthe-Sørenssen *et al.*, Phys. Rev. Lett. **83**, 764 (1999).
[27] H. Puhl, Physica A **197**, 14 (1993).